Interreg
ITALIA-SLOVENIJA
UNIONE EUROPEA
EVROPSKA UNIJA
NANO-REGION
Progetto strategico co-finanziato dal Fondo europeo di sviluppo regionale
Strateški projekt sofinancira Evropski sklad za regionalni razvoj

PROOF-OF-CONCEPT EXPERIMENT REPORT

SURFACE AND CROSS-SECTION ANALYSIS OF CARBON MEMBRANES COVERED WITH THIN ACTIVE CATALYST LAYER

Authors:

Gregor Kapun

CENN - Nanocenter

Jamova 39, 1000 Ljubljana, Slovenia

Mattia Fanetti

Materials Research Laboratory, University of Nova Gorica

Vipavska 11c, 5270 Ajdovščina, Slovenija

Nanocenter

Proof-of-Concept experiment details

Received sample: the company provided three different samples of carbon membranes covered with thin active catalyst layers.

Table 1: Samples delivered by the company

Sample name	Planned analysis
SFG44_Co - tested in GDE	FIB-SEM analysis, Ar^+ ion cross-section polishing + SEM analysis
KS44_Co - tested in GDE	FIB-SEM analysis
KS44_Cu - tested in GDE	FIB-SEM analysis

Figure 1: Image of the delivered samples

Planned analysis:

1st Binocular microscope inspection of delivered samples prior FIB-SEM sample preparation

2nd FIB-SEM cross-section preparation and initial cross-sectional analysis

3rd UHR-SEM imaging of sample surfaces and FIB cross-sections + EDX analysis of FIB cross-sections

4th Ar^+ polishing (one selected sample) followed by SEM-EDX analysis

Sample preparation:

FIB sample preparation: carbon membranes with active catalyst layer (PEM samples) were cut with razor blade to reduce sample size to 10x5 mm. Extracted sample pieces were glued to 45° pre-tilted FIB stubs with Ag adhesive so that the same sample could be analyzed at UHR imaging conditions from two perspective: 1) perpendicular to the surface and 2) perpendicular to the FIB prepared cross-section. The samples were not sputtered with any conductive layer (they were confirmed electron conductive) so that the surface and cross-section could be imaged in intrinsic state.

Ar^+ X-section polishing: sample of carbon membrane with active catalyst layer was embedded with resin between two glass pieces and subsequently glued directly on the cross-section polisher mount. After the polishing (before SEM/EDX analysis), the X-section has been coated with amorphous C (6 nm) by sputter coating system (PECS, Gatan, US).

Measurement author, dates and place:

FIB cross-section generation and initial cross-sectional/surface imaging of the delivered samples was performed by Gregor Kapun in time period from 13/12/2021 to 14/03/2022 at CENN - Nanocenter, Jamova cesta 39, SI-1000 Ljubljana, Slovenia. Analyses were performed with FIB-SEM Helios Nanolab 650 (Thermo Fisher, The Netherlands) equipped with SDD X-Max 50 EDX detector (Oxford Instruments, UK).

UHR-SEM imaging and EDX analysis of generated FIB cross-sections and sample surfaces was performed by Gregor Kapun in time period from 16/01/2022 to 03/04/2022 at CENN - Nanocenter, Jamova cesta 39, SI-1000 Ljubljana, Slovenia. Analyses were performed by UHR-SEM Verios G4 HP (Thermo Fisher, The Netherlands), equipped with SDD Ultim Max 65 EDX detector (Oxford, UK). Software for EDX analysis AZtec 4.3 (Oxford, UK).

Ar^+ ion cross-section polishing has been performed by Andraž Mavrič and Mattia Fanetti at University of Nova Gorica, Vipavska 11c, 5270 Ajdovščina, Slovenia. Cross-sections were performed by using instrument JEOL IB-09010CP Ar^+ (Jeol, Japan).

SEM/EDX analysis of the Ar^+ ion polished sample was performed by Gregor Kapun at CENN - Nanocenter, Jamova cesta 39, SI-1000 Ljubljana, Slovenia. Analyses were performed by UHR-SEM Verios G4 HP (Thermo Fisher, The Netherlands), equipped with SDD Ultim Max 65 EDX detector (Oxford, UK). Software for EDX analysis AZtec 4.3 (Oxford, UK).

Observation/processing conditions:

Generation of FIB cross-sections and initial cross-sectional analysis:

FIB cross-sections of carbon membranes with catalyst layer were fabricated after deposition of a platinum protective layer on the surface (first 0.3 µm thick layer with EBID at 2 kV, 0.8 nA, second 1,2 µm thick layer deposited with IBID at 30 kV, 0.40 nA). Subsequently, material in front of Pt protection was milled away with FIB (30 kV, 64 nA), by generating special ROI geometry which enable cross-sectional analysis to the depth of 60 µm without shadowing of imaging and EDX signals. Freshly exposed cross-sections were made with FIB at 30 kV and 21 nA by sequential reducing ion beam currents down to 2.5 nA in a final polishing step.

FIB-SEM imaging of surface and cross-section was performed at the following conditions:

- surface and cross-sectional imaging: beam energy 2 kV, probe current 13-50 pA, ETD, ICE or in-column TLD-SE detector
- surface and cross-sectional Z-contrast imaging: beam energy 2 kV with probe current 400 pA for the case of ETD-BSE and in-column TLD-BSE detector.

UHR-SEM imaging of sample surface and generated FIB cross-sections:

- UHR surface imaging: beam energy 2 kV, probe current 25-50 pA, WD = 4 mm, UHR U-mode; Images were acquired by using in column integrated TLD-SE, MD and ICD detector (SE, BSE and low-loss BSE).
- UHR imaging of FIB generated cross-sections: beam energy 2 kV, probe current 13 pA, WD = 2 mm, UHR U-mode; Images were acquired by using in column integrated TLD-SE, MD and ICD detector (SE, BSE and low-loss BSE).

Ar^+ cross-section polishing: performed by JEOL IB-09010CP, Ar^+ ion energy 5.5 KV; current: 140 μA; polishing time 4.5 hr. Stage swinging during polishing.

SEM/EDX analysis of FIB and Ar^+ ion generated cross-sections:

The point, area, linescan or mapping EDX analyses were performed with the following parameters:

- Quantitative and TrueMap EDX analysis: beam energy 5 kV, probe current 800 pA, process time (PT): 6, Live Time (LT): 60 s; Number of channels: 2048; for the case of mapping PT:6, Dwell Time (DT): 1500 ms, 1 frame (spectrum imaging),
- Detector energy quant optimization and beam measurement was done on Silicon standard following the same parameters as used in above-described EDX measurements.

EDX data processing was done in AZtec 4.3 software (Oxford, UK) by using TrueQ algorithm for elemental quantification while linescan and mapping data were processed with TruLine and TruMap algorithm, respectively.

Main aim:

The main aim of the POC experiment is to analyze the active catalyst layer morphology on both, the top surface as well as its cross-section and compare it between the samples to observe the differences. FIB approach is used to prepare the cross sections on all three samples. Using UHR SEM differences in catalyst layer porosity, carbon support and catalyst metal phase are compared. Lastly Ar^+-ion polishing is used to prepare X-section on one sample and evaluate this approach in comparison to FIB.

Results

1. Initial SEM analysis and generation of FIB cross-sections

Initially, electron microscopy (EM) prepared samples of the delivered carbon membranes with catalysts layer were SEM imaged in cross-sectional and top surface viewing angles as shown in Figure 2. This enabled first impression of sample surface morphology, catalyst layer distribution (in general) across the carbon membrane and served as determination of suitable, mechanically intact, locations for generation of clean FIB-cross sections.

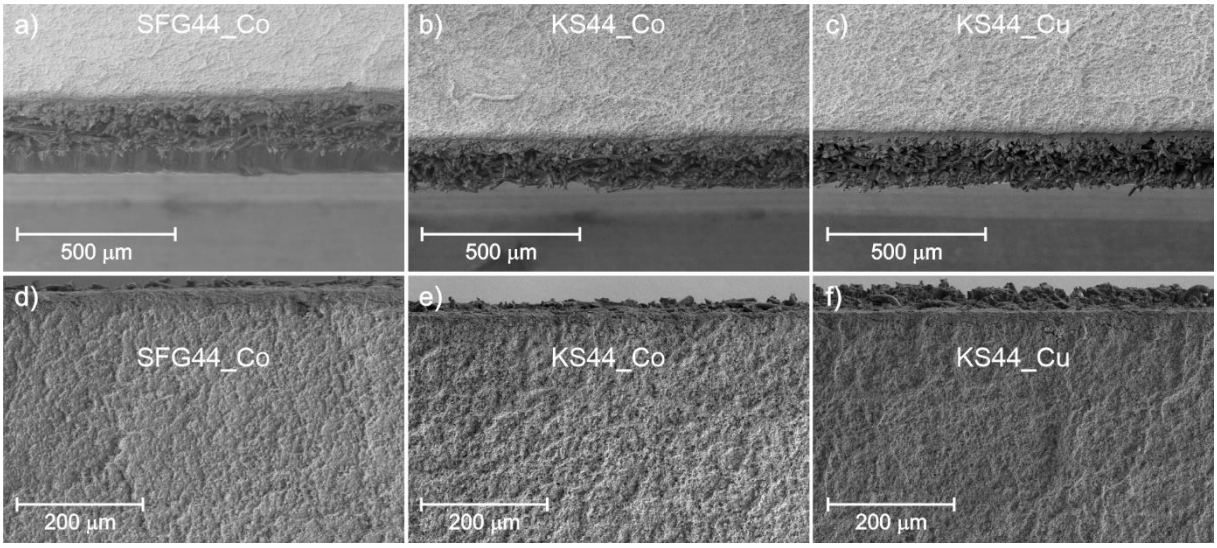

Figure 2: SEM images of EM prepared samples: SFG44_Co, KS44_Co and KS44_Cu mechanically cut carbon membranes with catalyst layer imaged in cross-sectional (a-c) and top surface viewing angles (d-f), respectively

Freshly generated FIB cross-sections of delivered samples with enlarged details at the surface are shown in Figure 3. In all three cases can be clearly seen supporting carbon membrane matrix which continues with porous gas diffusion layer-GDL (25-50 µm thick) upwards until smooth sub-surface ending and ends with active catalytic layer with maximum thickness up to ~6 µm.

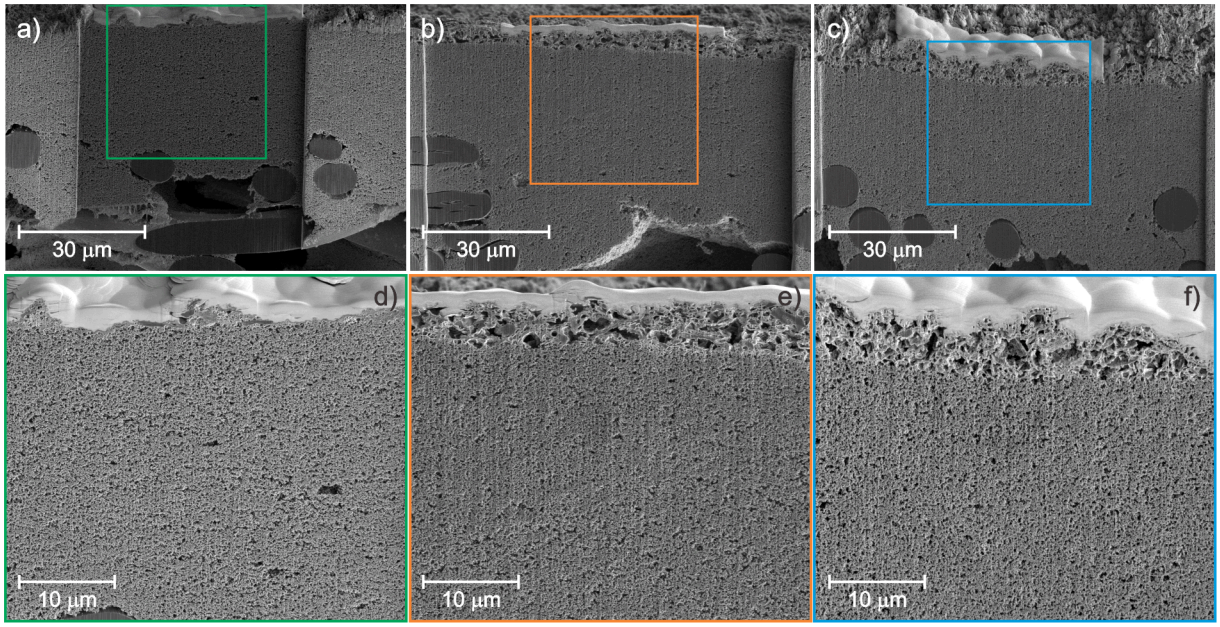

Figure 3: Freshly generated FIB cross-sections of carbon membranes with catalysts layer for a) SFG44_Co, b) KS44_Co and KS44_Cu samples with the corresponding enlarged details (d-e).

When zooming in to the catalyst layer (Figure 4), it can be seen in all three samples the GDL on the bottom of the images, catalyst layer in the middle and protective Pt layer on the top. The thickness of the catalyst layer for sample SFG44_Co appears to be varying between 150 nm and 4.4 µm, whereas with KS44_Co and KS44_Cu samples it appears to be more homogeneous, measuring between 3-6 µm. Moreover, in case of SFG44_Co, the catalyst layer appears to be porous only on the thicker part of the catalyst layer, whereas on the thinner part it does not appear to be porous. In contrast, the catalyst layers of KS44_Co and KS44_Cu samples appear to contain a high level of porosity which should in principle allow much better transport of gaseous species to and from the active catalyst sites.

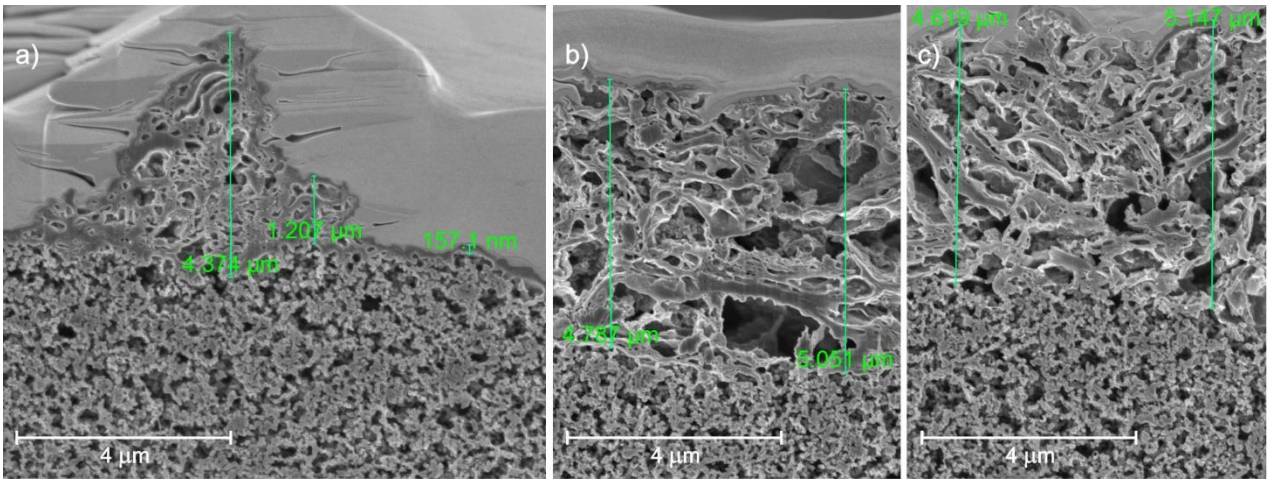

Figure 4: Catalyst layer cross-section comparsion between (a) SFG44_Co, (b) KS44_Co and (c) KS44_Cu.

2. UHR-SEM analysis of catalyst layer surfaces

Imaging of catalyst top layer surfaces reveals major differences in homogeneity as well as morphology between the samples. At lower magnification in case of SFG44_Co (Figure 5a) the catalyst layer looks a lot more rough than in case of samples KS44_Co and KS44_Cu (Figures 5b,c respectively). Moreover, when observing the surface at higher magnification (Figures 5d-f) in case of SFG44_Co (Figure 5d) it can be observed that the catalyst layer is in some parts very thin where almost no material is deposited and on some spots, larger chunks of material are present. Additionally, it can be observed that in case of KS44_Cu (figure 5f) the primary particles of the catalyst composite are the smallest among the three samples.

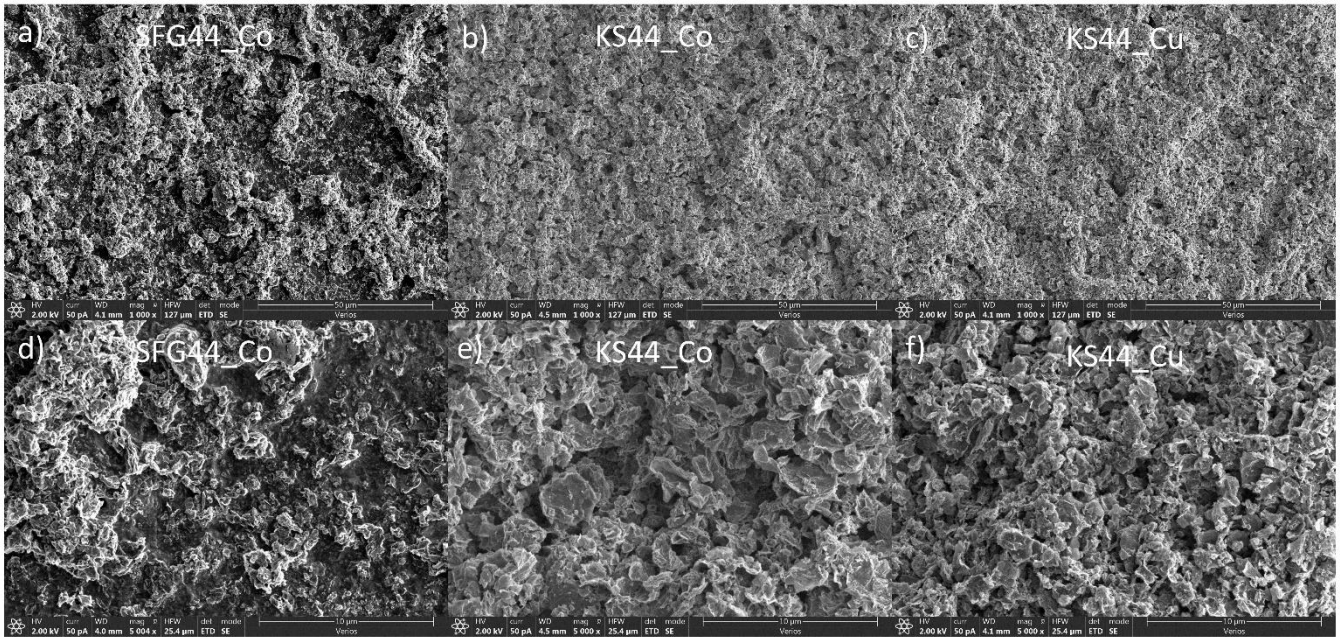

Figure 5: SEM images of top surface morphology (a-f) at different magnifications for samples: SFG44_Co, KS44_Co and KS44_Cu.

Looking at higher magnification (Figures 6a-c) the difference in the carbon morphology can be observed, where in case of SFG44_Co (Figure 6a) the carbon support material looks less defined, and it appears to be glued together more with proton conductive ionomer-Nafion. In case of KS44_Co and KS44_Cu (Figures 6b, c) the carbon support appears to have a more layered structure. UHR-SEM phase contrast analysis based on the detection of low-loss back scattered electrons, in particularly by using in-column MD detector, (Figures 6 d-f) reveals the active catalyst sites. In all three samples the catalyst distribution seems homogeneous over the carbon support, in case of KS44_Co and KS44_Cu (Figures 6d, f) slightly better than with SFG44_Co (Figure 6d). Moreover, in contrast to the SE detector the MD detector allows for excellent nanoparticle detection which allows for great analysis of the metal phase of the catalyst.

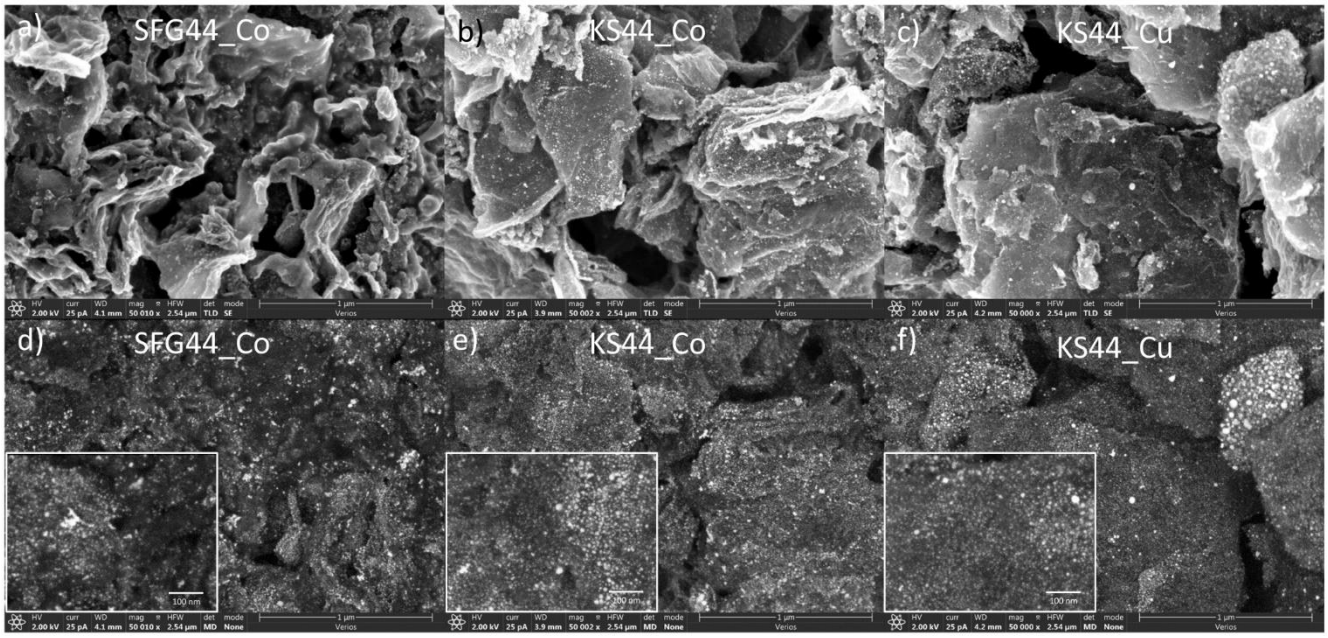

Figure 6: UHR SEM images in SE mode (a-c) and MD mode (d-f) for samples: SFG44_Co, KS44_Co and KS44_Cu.

3. UHR-SEM and EDX analysis of FIB generated cross-sections of catalyst layer

Cross-sections of the catalyst layer generated by FIB (Figures 7a-c) when observed with UHR-SEM give an excelent insight into the morphology and structure of the catalyst layer. Great differences can be observed between the samples as mentioned in section 1 in regards to the thickness of the catalyst layer as well as its porosity.

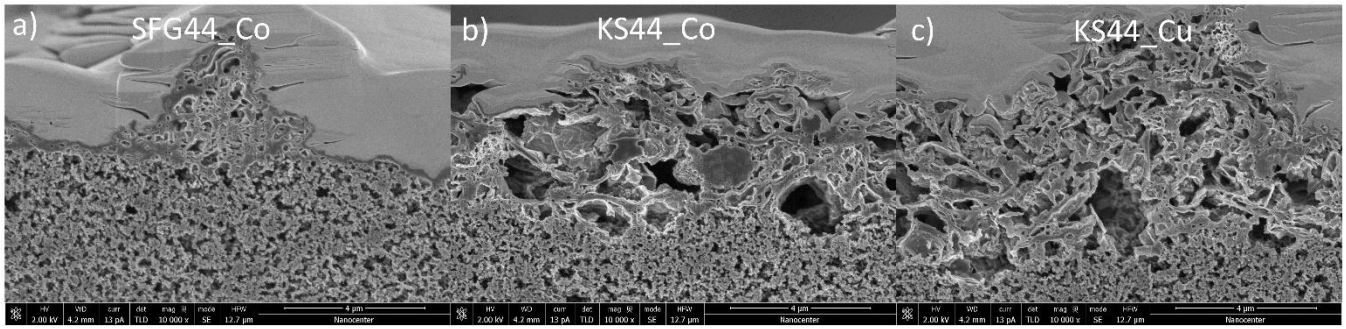

Figure 7: Cross-section images (a-c) for samples: SFG44_Co, KS44_Co and KS44_Cu.

When zooming in further additional details are revealed (Figure 8). In case of SFG44_Co sample (Figure 8a), the contact of the catalyst layer with the porous carbon layer of the GDL appears to be more glued together with ionomer than in the case of KS44_Co (Figure 8b) and especially KS44_Cu (Figure 8c). Moreover, the difference in thickness of the catalyst layer between SFG44_Co and other two samples can be more profoundly observed. Using the MD detector (Figures 6 d-f), it again reveals the active catalyst sites which are present in the catalyst layer.

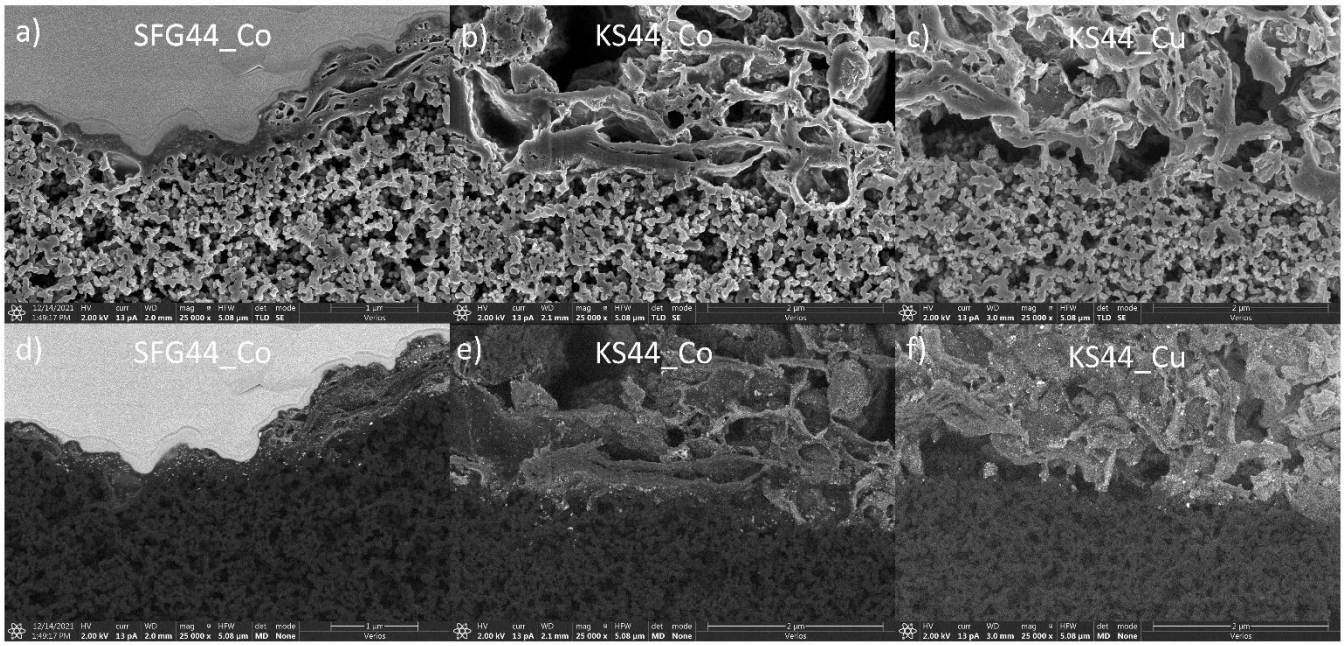

Figure 8: UHR-SEM cross-sectional images in SE mode (a-c) and MD mode (d-f) for samples: SFG44_Co, KS44_Co and KS44_Cu.

Complementary to above-described phase contrast images, EDX mapping analysis enables evident insight into elemental distribution along cross-sections. The use of low kV EDX TrueMap (5 kV) analysis allows detection of characteristic X-ray lines from smaller analytical volume. Therefore, all the present elements within cross-section can be properly identified according to their K, L or M line. EDX TrueMap analysis of samples SFG44_Co, KS44_Co and KS44_Cu along freshly exposed FIB generated cross-sections are presented in Figure 9, Figure 10 and Figure 11, respectively. Based on the Z-contrast image, and individual elemental maps we could effectively determine gas diffusion layer (GDL) and catalyst layer as well as potential diffusion of individual components between them. Moreover, with reprocessing EDX spectra (by subtracting signal background and spectrum deconvolution) we could even detect clusters of fine catalyst particles. This approach enabled analytical insight into distribution of catalysts and Nafion ionomer components within catalyst layer. For all three samples GDL layer was identified as porous carbon (C K line) while catalyst layer composition was found as Pt/Co or Pt/Cu active catalysts + carbon, oxygen and fluorine related to catalyst supporting matrix and Nafion ionomer. For clarification it is also important to note that each individual Pt TrueMap analytical image include highly intense Pt layer (dented with red marker) at the very top of catalyst layer which correspond to dense FIB deposited Pt protection film, required for generation of finely polished FIB cross-sections. The later can be clearly verified by Z-contrast and Layered EDX Truemap image included in the Figures.

TrueMap analysis of SFG44_Co (Figure 9) confirms that active catalysts particles are composed of Pt/Co where both elements were found homogenously distribute within catalysts layer (Figure 9c, Figure9d). Complementary to above-described UHR-SEM results, the catalysts layer appears to be less porous, especially in the thinnest areas at the contact with GDL layer, which can be seen in Figures 9a, Figure 9f and Figure 9g. Nafion ionomere in SFG44_Co appears to be accumulated at the bottom of catalytic layer and there is no trace of fluoride diffusion into GDL layer as evident in Figure 9e.

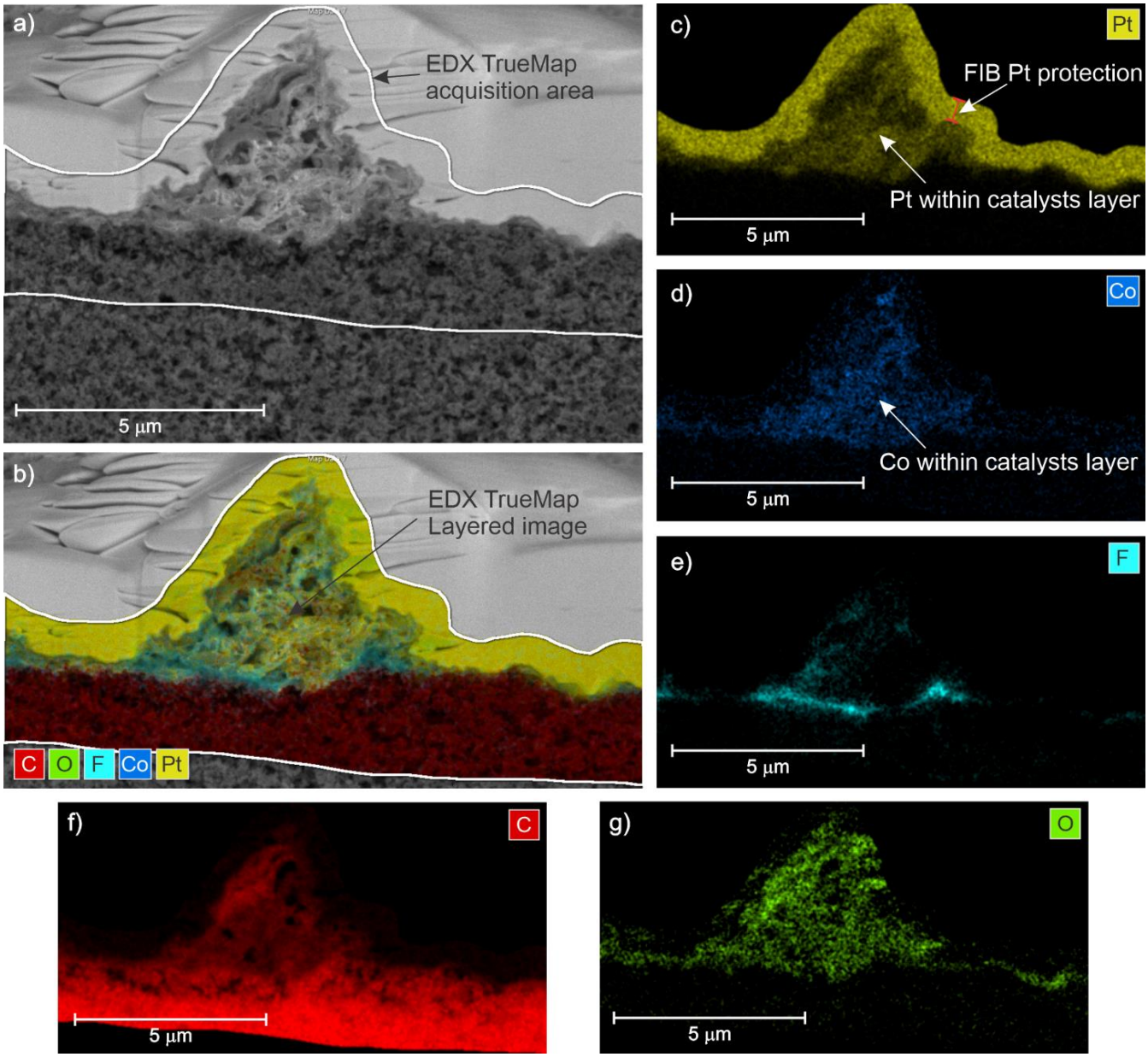

Figure 9: EDX TrueMap analysis of sample SFG44_Co along FIB generated cross-section: a) Z-contrast image with denoted EDX TueMap acquisition, b) EDX TrueMap image layered image, c) Pt individual map (Pt Mα), d) Co individual map (Co Lα), e) F individual map (F Kα), f) C individual map (C Kα), g) O individual map (O Kα).

TrueMap analysis of KS44_Co (Figure 10) again confirmed that active catalysts particles were composed of Pt/Co where both elements were found homogenously distributed within catalysts layer except in the case of Pt/Co agglomerate which is denoted in Figure 10c and Figure10d. By the contrast to SFG44Co, the catalyst layer in KS44_Co appeared thicker and significantly more porous which can be seen in Figures 10a, Figure 10f and Figure 10g. Nafion ionomer in KS44_Co was found in generally distributed across entire catalytic layer, however in this case diffusion of fluoride from catalytic layer into GDL layer was noted which can be seen in Figure 10e.

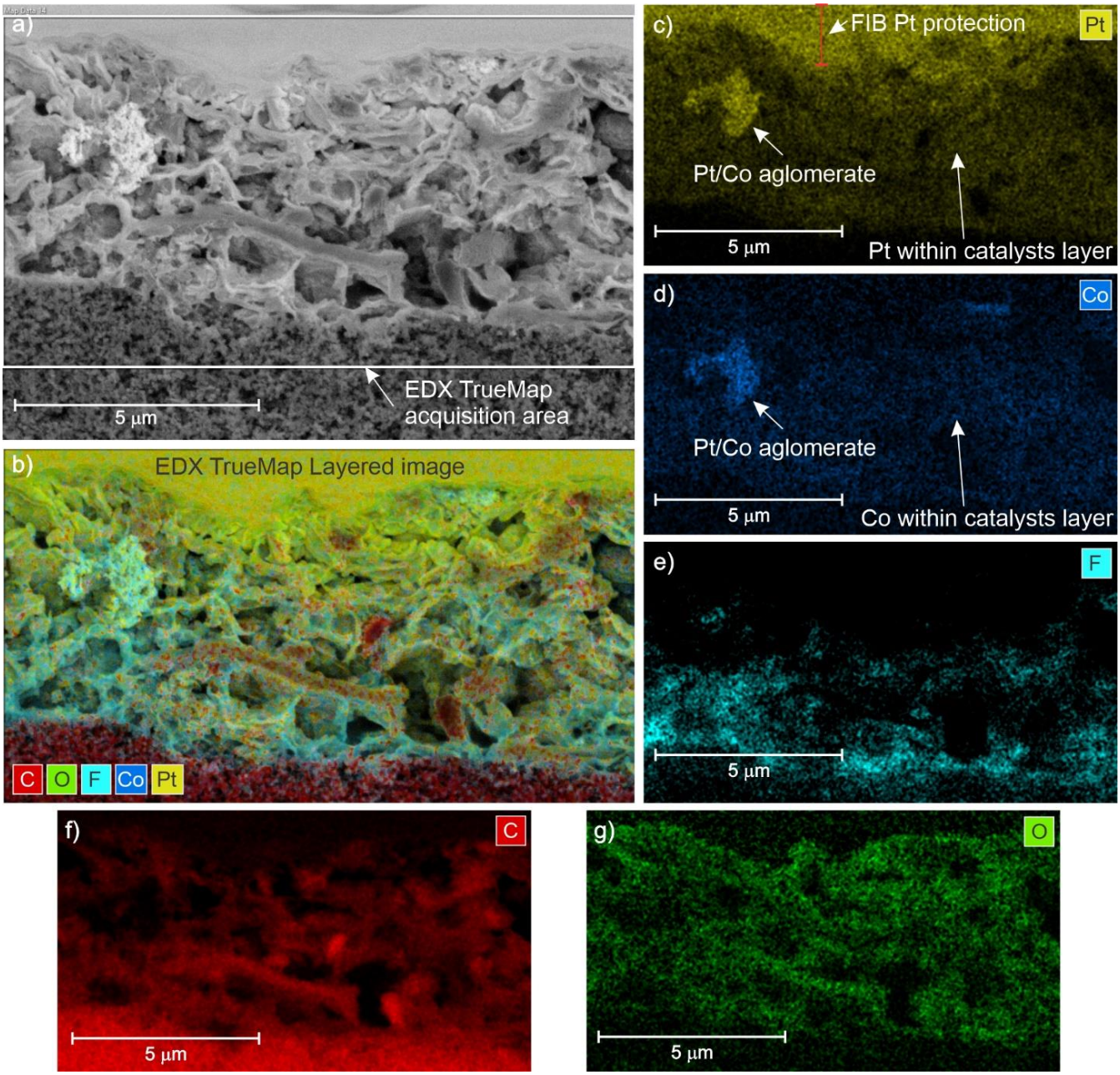

Figure 10: EDX TrueMap analysis of sample KS44_Co along FIB generated cross-section: a) Z-contrast image with denoted EDX TueMap acquisition, b) EDX TrueMap image layered image, c) Pt individual map (Pt Mα), d) Co individual map (Co Lα), e) F individual map (F Kα), f) C individual map (C Kα), g) O individual map (O Kα).

TrueMap analysis of KS44_Co (Figure 11) confirmed that the active catalysts particles were composed of Pt/Cu where both elements were found homogenously distributed within catalysts layer. In this sample the catalyst also appeared thicker and significantly more porous (in contrast to SFG44_Co) which can be concluded from Figures 11a, Figure 11f and Figure 11g. Nafion ionomer in KS44_Cu was found distributed in the bottom half of catalytic layer and in this case the most intense diffusion of fluoride from catalytic layer into GDL layer was detected which can be seen in Figure 11e.

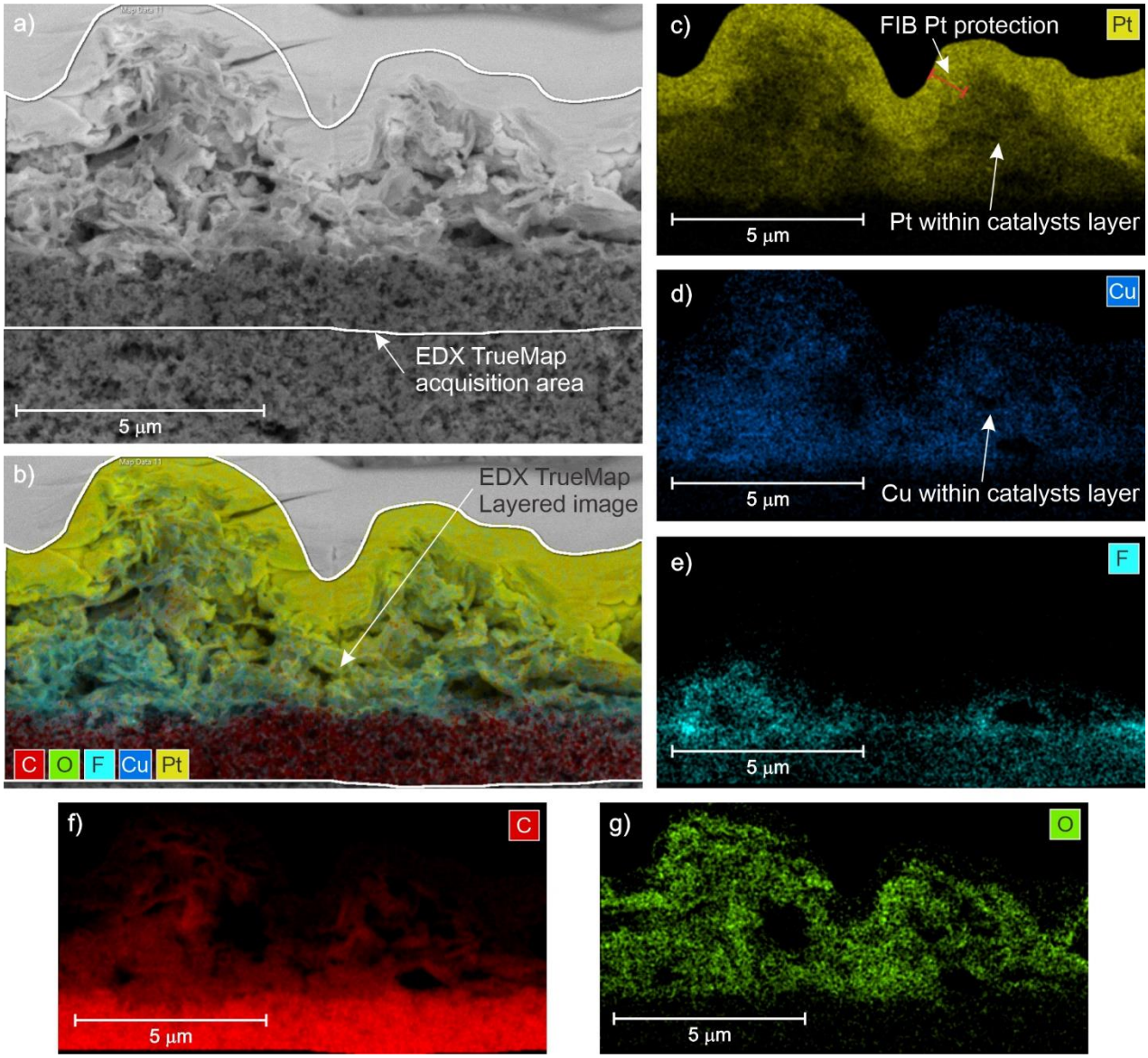

Figure 11: EDX TrueMap analysis of sample KS44_cu along FIB generated cross-section: a) Z-contrast image with denoted EDX TueMap acquisition, b) EDX TrueMap image layered image, c) Pt individual map (Pt Mα), d) Co individual map (Co Lα), e) F individual map (F Kα), f) C individual map (C Kα), g) O individual map (O Kα).

4. SEM-EDX analysis of Ar^+ ion polished cross-section of full carbon membrane including catalytic layer

Prior generation of a large Ar^+ ion polished cross section, the chosen sample SFG44Co was sandwiched between two glasses and infiltrated with epoxy resin. This step was mandatory to mount the sample to stub and protect the catalytic layer surface against broad Ar^+ ion beam. Low magnification SEM image in Figure 12a shows the obtained large cross-section where aprox. 1.4 mm wide area of catalytic ad GDL layer was successfully polished and exposed for SEM-EDX analysis. As denoted in Figure 12a the sequence of components in top-down direction is as follows: Protecting objective glass, resin, catalysts layer, gas diffusion layer (GDL), carbon membrane, resin and supporting glass. Figure 12b presents Z-contrast image large cross-sectional area of sample SFG44 where catalytic layer can be seen (brightest contrast) in much wider statistics compared to limitations of FIB generated cross-section (~70 μm). Enlarged detail of catalytic layer is shown in Figure 12c. In the later can be seen that epoxy resin is not present only on the top of sample but has been also infiltrated into porous structure of catalytic layer as well as in GDL and carbon membrane. In this case we can not guarantee if the porous structure of catalyst layer was not modified during sample preparation due to the epoxy resin infiltration. Apart of that, the exposed cross-section is smooth and free of mechanically damage so it can be used for SEM and EDX analysis across entire length exposed cross-section.

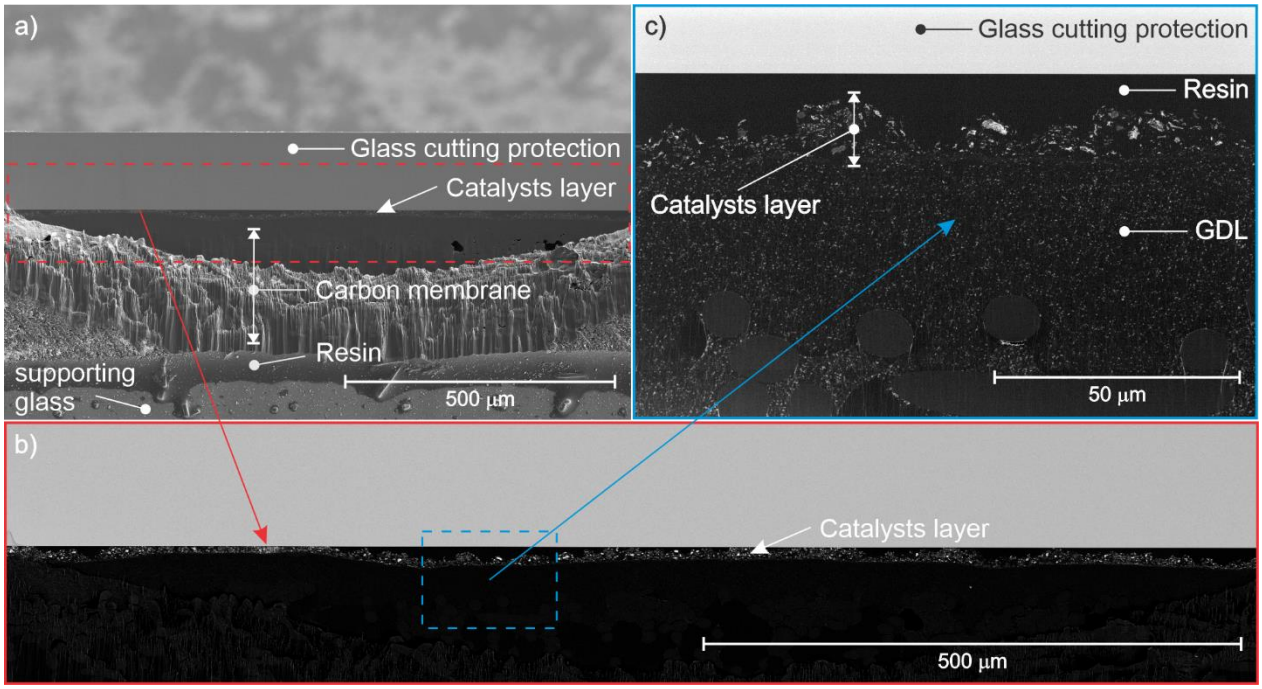

Figure 12: SEM images of sample SFGCo_44 large area cross-section generated by Ar^+ cross-section polisher

EDX TrueMap analysis of large Ar^+ ion polished cross-sectional area for the case of sample SFG44Co is shown in Figure 13. Complementary with results obtained on FIB generated cross-sections, it was possible to identify that the active catalytic particles were composed of Pt/Co metals also in the case of Ar^+ ion polished cross-sections. In general, both metals appear homogenously distributed along catalysts layer as shown in Figure 13c and Figure 13d. However, here is important to note that EDX TrueMap results shown different impression compared to results obtained on FIB generated cross-sections, since in the latter case pores within catalysts layer were infiltrated with resin. Therefore, open pores within catalyst layer were filled with artificial phase (which contains C and O elements) and EDX signals of Pt and Co were acquired in one single imaging plain. As a grater benefit, EDX

TrueMap analysis of Ar^+ ion cross-section was acquired at higher resolution across larger statistical area and therefore we could detect even several Pt/Cu agglomerates where Co analytical images represent highest intensity can be seen in Figure 13d. Moreover, Pt elemental distribution within catalytic layer could be clearly distinguished since sample was embedded in epoxy. As a drawback of Ar^+ ion prepared cross-section, we could not properly identify fluorine X-ray signal since cross-section was slightly contaminated with barium which originates from glass protection on top of the sample. Namely barium Lα line directly overlaps with fluorine Kα line therefore it was not possible to separate these elements in TrueMap analysis.

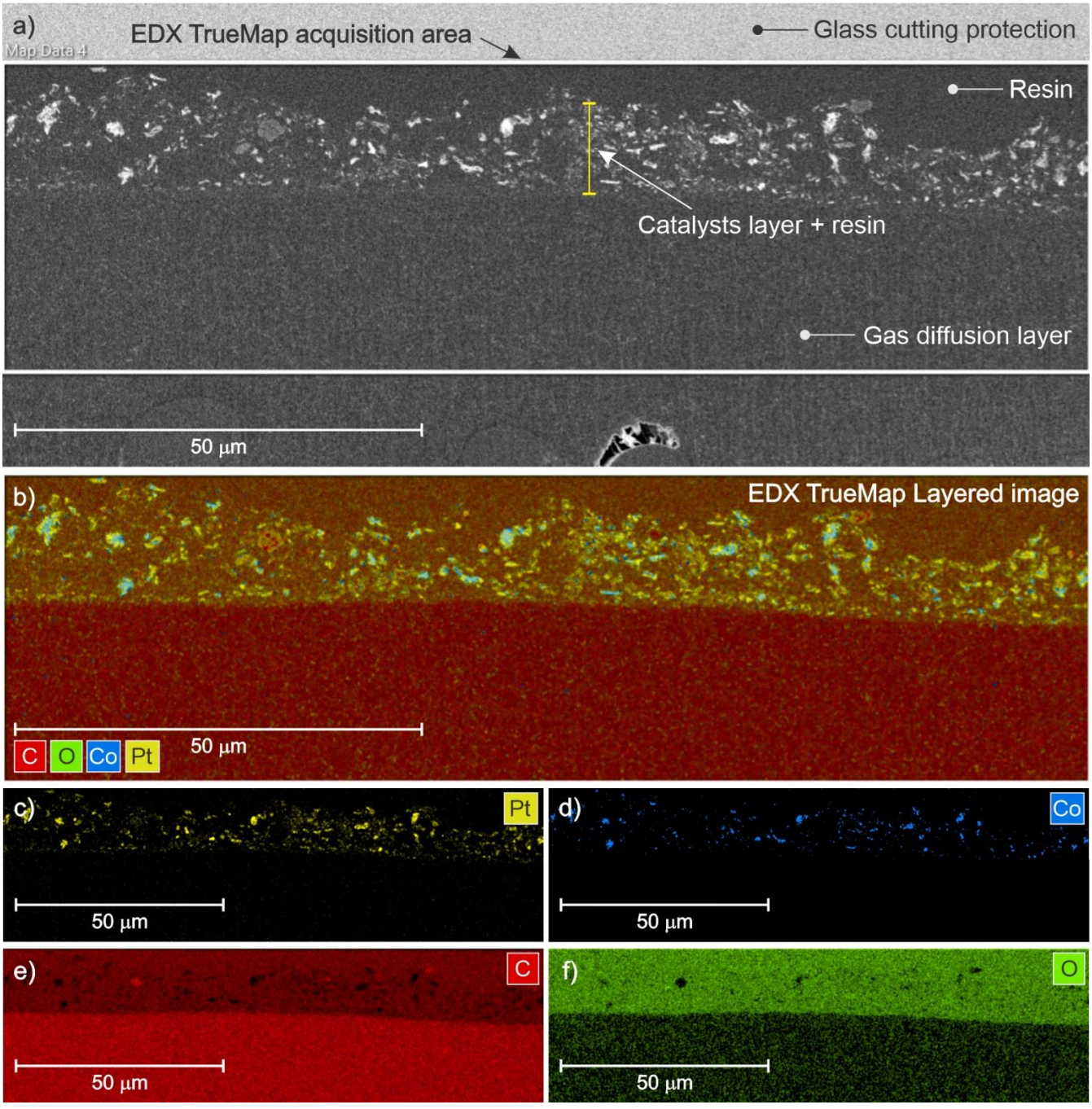

Figure 13: EDX TrueMap analysis of sample SFG44_Co along large Ar^+ ion polished cross-section

Concluding remarks on the capabilities of the demonstrated techniques

With focused ion beam (FIB) it is possible to obtain intrinsic, mechanically damage free, cross sections on carbon membranes covered with thin active catalyst layer. Protection of sample surface with electron beam induced Pt deposition preserves catalyst layer surface and enable smooth and clean cross-section suitable for low voltage SEM imaging at high magnification. With the FIB approach we can precisely select site specific location of cross-section, however this method presents two major drawbacks: 1) it is not possible to cut throughout entire sample membrane (>150 mm thickness) in a reasonable time and 2) the fabricated cross-section area is significantly smaller compared to Ar^+ ion polished cross-section (in the case of Ga-FIB typically limited to 80 μm in width and 40 μm in depth).

By Ar^+ ion milling it is possible to easily generate a large cross-sectional area throughout entire carbon membrane. Prior milling membrane sample must be sandwiched between two harder materials (i.e. glass) and embedded in resin. The obtained cross-section is smooth enough to easily resolve all the features, down to resolution limit of the used SEM technique. The shortcomings in the use or Ar^+ ion milling is: 1) the poor capability in localizing the cutting plane (the accuracy in the positioning of the shield for cutting is approximately 50 μm), 2) by embedding the sample within resin, the porous structure of catalytic layer may be artificially modified.

Once the cross-section is generated SEM analysis allows inspection of components morphology, porosity, shape and size of particles/agglomerates, contacts between the layers and phase distribution. In addition, EDX analysis allows to identify main components and elemental composition of features. The use of low beam energy (5 KeV) enables improved lateral resolution in the elemental maps, with possibility to resolve details of ~200 nm. However, at low beam energy the overlapping between emission lines becomes a frequent issue, and an effective software (like the one used here) for the deconvolution of maps is necessary to achieve correct datasets. The use of UHR-SEM with several in-column detectors allows in principle imaging of finest particle (below 1 nm) and simultaneously detection of nano-compositional phase differences by collection low-loss back scattering electrons. By using 2 kV acceleration voltage and simultaneously acquisition of in-column SE and in-column MD detector we could easily image and resolve (in high contrast difference) even 1-2 nm Pt/Cu or Pt/Co catalytic particles within catalyst layer matrix.

Further advices

Cross section analysis gives a very promising insight into the catalyst layer, and it might provide even more precise information if tomography imaging would be utilized. In this way the 3D structure could be obtained and also some closed porosity revealed. Moreover, with different detectors, various properties could be observed. For instance, with SE detector mainly porosity of the layer could be assessed and with MD detector, distribution of the nanoparticles could be assessed within the given volume of interest. In combination with EDX analysis this approach could be a really powerful tool for characterization of the catalyst layers.

This report has been written by Gregor Kapun and Luka Pavko (28/07/2022)